UNIVERSITÀ DEGLI STUDI DI PADOVA

Dipartimento di Fisica e Astronomia "Galileo Galilei"

Corso di Laurea in Fisica

Tesi di Laurea

The Memory Effect of Gravitational Waves in General Relativity: Theoretical overview and observational perspectives

Relatore

Prof. Jean-Pierre Zendri

Correlatore

Dr. Antonello Ortolan

Laureando

Andrea Moscatello

Anno Accademico 2018/2019

Contents

Abstract

The aim of this thesis is to carry out the study of the memory effect of gravitational waves (GWs). The first chapter is a brief introduction to General Relativity (GR), gravitational waves and their detection. The second chapter is dedicated to a theoretical description of the memory, with its analytical form and its possible sources. Both the linear and the non-linear effects are described, along with their differences in sources and physical interpretations. I will show how these two different effects appear to be the same when considering GWs as massless gravitons. I will also show how to compute the memory for a black holes (BHs) merging. The last chapter deals with perspectives on the memory detection: an analysis of its detectability and its signal to noise ratio (SNR) with the aLIGO and aVIRGO detectors. I will also give an analytical form for the aVIRGO noise expected for the O3 run. Eventually, I will focus on detection via summation of multiple memories and the orphan memory, a memory detected without parent GW signal.

Introduction

From their first detection on 14th September 2015 [1], and throughout the following detections, the study of gravitational waves has become one of the main topic in modern physics. GWs were predicted by Einstein's General Relativity 100 years ago, and now they are the latest successful test of this theory, which still holds up without flaws. In addition to being a milestone for both theoretical and experimental physics, GWs also provide us a new powerful tool to look at the universe. Before GW150914 detection, astrophysical studies were made through electromagnetic waves. However, the universe can be opaque for light: indeed photons can be scattered and stopped by masses, for example interstellar dust. Contrariwise, gravitational waves propagate through any region of the universe essentially unperturbed. Huge steps forward were made, for example, in the study of black holes. With the detection of couples of black holes merging, we gained an impressive amount of new information on those compact bodies (their spatial distribution in the universe, distribution of spins and masses, etc...) just by looking at the emitted GW's waveform.

GWs have lots of undiscovered theoretical aspects that have not been elaborated until now because of the lack of experimental evidence. One of them is the *memory effect* [2]: a permanent displacement in relative position between two ideal free falling masses, i.e. a permanent perturbation of spacetime. After a GW has passed, spacetime is assumed to come back to its initial flat state. However, after a GW along with its memory effect has passed, it causes a permanent deformation: it leaves a "memory" of its passage.

Gravitational-wave memory comes in two kinds: the linear and the non-linear memory. The linear memory has been known since the 1970's (see Ref. [3], [4] and references therein) and arises from sources that produce a net change in the time-derivatives of their quadrupole moment. An example of a source with linear memory is an hyperbolic orbit. Other examples of linear memory are systems that change from being bound to unbound (or vice versa). For instance, binaries whose members are captured, or loses mass. The nonlinear memory was discovered independently by Blanchet and Damour [5], and Christodoulou [6]. It is often referred to as the "Christodoulou memory". The nonlinear memory is present in every GW event, and arises from the stress-energy flux carried by the original GW. It can be interpreted as the GWs generated by the GW itself. In a BHs or neutron stars (NSs) coalescence the two bodies are gravitationally bound throughout all the event, so with these binaries the nonlinear memory is the only contribution expected. Indeed, in this thesis I will focus on the computation of the nonlinear memory sourced by BHs mergings.

The detection of a memory in spacetime will constitute a new test of the full theory of General Relativity, and will improve our knowledge of the universe. One of the firsts application is the BHs merging parameters estimation. After the detection of a GW, different templates are matched to the signal, and the one with the best compatibility gives the best estimate of the binary parameters: masses, spin, distance and so on. If our signal has a memory component and our template does not take into account this feature, the best fitting parameters will be biased by our error, and so they will not be the correct ensemble of parameters for the binary coalescing system.

On the theoretical side, the memory effect can also be used in quantum gravity searches: it can be shown that the memory is heavily suppressed in theories with a spacetime with more than 4 non-compact dimensions and it also gives stringent boundaries to the graviton mass [7].

On the experimental side, a huge effort is being made in upgrading the existing GW detectors, LIGO in US and Virgo in Italy. The new generation of interferometers, under the name of Advanced LIGO (aLIGO) and Advanced Virgo (aVIRGO), will soon start new scientific runs with an incredibly high sensitivity $S_h \simeq 3.5 \times 10^{-24}$ in the [100-600] Hz range of frequencies (for aLIGO) [8] [9] [10]. I will give an analytical form for the expected noise of the aVIRGO detector in the O3 run.

In this thesis I focus on GW memory detection in order to provide some estimate of GW memory waveforms for different systems, and I study some aspects of the structure of the resulting gravitational waves templates. Some estimations of detectability of memory effects in aLIGO and aVIRGO detectors are eventually given.

Chapter 1

General Relativity overview

In this chapter I will give a brief introduction to the basic concepts of space, time and gravity in general relativity. Then I introduce GW and the study of their physical effects. In particular I will focus on GW memory effect which is the scope of this thesis.

1.1 Space, time and gravity

1.1.1 Newton's theory

Before starting with Einstein's theory of relativity it is useful to look back on the space and time concepts of classical physics and their application in classical mechanics.

Space and time

The concepts of space and time, as two separated entities, where first proposed in classical philosophy and were taken as foundations of Newton's theory of gravity. Newtonian theory rests on the assumption that there is an absolute time that flows at the same rate for any observer. The physical space is modeled as a 3-dimensional euclidean space where events take places. Space and time are two very different entities. In particular, if we consider the two separated points $(t_a; x_a, y_a, z_a)$ and $(t_b; x_b, y_b, z_b)$, and the corresponding two events considering also the time at which they take place, the differences:

$$\Delta l = \sqrt{(\Delta x)^2 + (\Delta y)^2 + (\Delta z)^2} \tag{1.1}$$

$$\Delta t = t_b - t_a, \tag{1.2}$$

are invariant under galilean transformations:

$$\begin{aligned} t' &= t \\ x' &= x - v_x t \\ y' &= y - v_y t \\ z' &= z - v_z t. \end{aligned} \tag{1.3}$$

Galilean transformations are used to transform between the coordinates of two reference frames which differ only by a constant speed motion. The invariance of time can be seen from the first equation of the set. From the two separated "distances" in (1.1) and (1.2) it follows that space and time are two mathematically and physically separated entities.

Qualitatively, these two entities are immutable: we can't change time flow rate nor we can bend or stretch space. They are two solid structures which, regardless every physical action we can do, will

never be modified. As we will see later, those ideas do not hold anymore when considering a relativistic regime.

Gravity

Newton interpreted gravity as a force acting between two (point-)massive objects A,B; and it is expressed with his famous law of universal gravitation

$$\vec{F} = -G\frac{m_1 m_2}{r^2}\vec{e}_{AB}, \tag{1.4}$$

where m_1 and m_2 are the masses of the two bodies considered, r is the distance between them, $\vec{e}_{AB}$ is the unit vector pointing from A to B and $G = 6.67 \times 10^{-11}$ $\mathrm{m^3 kg^{-1} s^{-2}}$ is the gravitational constant. This force acts instantly on both A and B, and this, as we will see, violates Einstein's postulate that c is the maximum speed at which something can travel or propagate. This theory can therefore only be an approximation to a yet more fundamental theory. It is important to note that here gravity is an actual force: two bodies attract each other like two opposite electrical charges do. This means that, in Newton's theory, there is no connection between the force and the geometry of space. Gravity is an action at distance: two bodies attract each other without any physical touch or mechanical contact. This force is a nonlocal interaction of objects that are separated in space.

1.1.2 Einstein's theory

Through his works in 1905 (Special Relativity) and 1915 (General Relativity) Einstein radically changed the viewpoint on both space and time, and also gravity.

Spacetime

In special relativity (SR) Einstein abandoned the assumption of an absolute time and replaced it by postulating that c, the speed of light in vacuum, is the same for all observers, regardless the motion of the light source. Now if we consider two different inertial frames S and S' and we want to connect an event in the first frame with the same event in the second one we can not use galilean transformations. The transformations we must use are *Lorentz transformations*, also known as "boosts". For example, a boost along the x axis is

$$\begin{aligned} ct' &= \gamma(ct - \beta x) \\ x' &= \gamma(x - \beta ct) \\ y' &= y \\ z' &= z, \end{aligned} \tag{1.5}$$

where $\beta = v/c$ and $\gamma = 1/\sqrt{1-\beta^2}$. v is the relative speed of the two frames.

Let us now consider two events A and B with coordinates (t_a, x_a, y_a, z_a) and (t_b, x_b, y_b, z_b). It can be shown that the interval

$$\Delta s^2 = -c^2\Delta t^2 + \Delta x^2 + \Delta y^2 + \Delta z^2 \tag{1.6}$$

is invariant under Lorentz transformations. The mixing of space and time coordinates in Δs and in Lorentz boosts, as supported by Minkowski's idea, suggests that space and time are actually linked. In fact, they stop being two separated entities and they bond together, forming a four-dimensional continuum: the *spacetime*.

Gravity as geometry

When trying to add acceleration and mass to SR, Einstein had a dramatic viewpoint changing idea. Given that every free body on Earth starts falling down with the same acceleration, regardless of its mass, there is no actual force pulling them down. Instead, they slide down because of a curvature on spacetime surrounding them. In other words: if spacetime under an object is bent, the latter follows this curvature, nothing pulls it down. Gravity is no more a mere force, it is manifestation of the geometry of spacetime.

Let us define with x^μ the four-vector of the spacetime coordinates of an event

$$x^\mu \equiv (x_0, x_1, x_2, x_3). \tag{1.7}$$

In a generic Riemann manifold we can express the interval between two points as

$$ds^2 = g(x)_{\alpha\beta} dx^\alpha dx^\beta, \tag{1.8}$$

where $g(x)_{\alpha\beta}$ is called the *metric tensor*. If we consider spacetime coordinates we can see that, writing $x^\mu = (ct, x_1, x_2, x_3)$, the element Δs^2 in (1.6) is formally in the same form of a generic segment (1.8):

$$\Delta s^2 = \eta_{\alpha\beta} dx^\alpha dx^\beta, \tag{1.9}$$

where $\eta_{\alpha\beta}$ is the Minkowski metric tensor, defined as[1]

$$\eta_{\alpha\beta} = \begin{pmatrix} -1 & 0 & 0 & 0 \\ 0 & 1 & 0 & 0 \\ 0 & 0 & 1 & 0 \\ 0 & 0 & 0 & 1 \end{pmatrix}, \tag{1.10}$$

and it describes a flat spacetime. How can we quantify the curvature of spacetime? The specific geometric structure that allows us to do so is the *curvature tensor*

$$R^\alpha_{\lambda\delta\theta} = \partial_\delta \Gamma^\alpha_{\lambda\theta} - \partial_\theta \Gamma^\alpha_{\delta\lambda} + \Gamma^\alpha_{\delta\gamma}\Gamma^\gamma_{\lambda\theta} - \Gamma^\alpha_{\gamma\theta}\Gamma^\gamma_{\delta\lambda}, \tag{1.11}$$

where $\Gamma^\delta_{\alpha\gamma} = \frac{1}{2} g^{\beta\delta}(\partial_\alpha g_{\beta\gamma} + \partial_\gamma g_{\alpha\beta} - \partial_\beta g_{\alpha\gamma})$ is the Christoffel symbol. It actually gives us a measure of how much spacetime is curved. Now that we can quantify the curvature of spacetime from its metric tensor, we will see how it is actually linked to the presence of a massive object.

1.2 Einstein's equations

The connection between mass (or energy) distribution and spacetime curvature is expressed in the famous Einstein's equation

$$R_{\mu\nu} - \frac{1}{2} g_{\mu\nu} R = \frac{8\pi G}{c^4} T_{\mu\nu}, \tag{1.12}$$

where $R_{\mu\nu} = R^\gamma_{\mu\gamma\nu}$, $R = R^\alpha_\alpha$, and $T_{\mu\nu} = \rho_0 u_\mu u_\nu$ is the *stress-energy tensor* of the energy/matter fields, which describes their density or flux of energy and momentum. These equations are a set of 10 differential equations with a clear meaning: as the right hand term describes the energy in a given point of spacetime (or a flux of energy, etc...), the left hand term describes the curvature in that point. The connection between the two is mathematically determined.

[1] It is both accepted to write the Minkowski metric tensor as diag(-1,1,1,1) or diag(1,-1,-1,-1), throughout all the thesis I'll use the first convention

1.3 Gravitational waves

Solving equation (1.12) is anything but easy. However, if we are in the newtonian (or weak-field) approximation I can write our metric tensor as

$$g_{\mu\nu} = \eta_{\mu\nu} + h_{\mu\nu},$$

with $|h_{\mu\nu}| << 1$ (spacetime is approximately flat, but with a perturbative term: $h_{\mu\nu}$). I can assume that our metric tensor can be described as $g_{\alpha\beta} = (flat) + (perturbation)$. The perturbative term, h, is the one interested by gravitational waves. Given that $|h_{\mu\nu}| << 1$, I can linearize in $h_{\mu\nu}$ Einstein's equations (1.12) and defining the *trace-less* $\overline{h}_{\mu\nu} \equiv h_{\mu\nu} - \frac{1}{2}\eta_{\mu\nu}h$, with $h \equiv h^{\alpha}_{\alpha}$, we obtain:

$$\Box\overline{h}_{\mu\nu} + \eta_{\mu\nu}\partial_\rho\partial_\sigma\overline{h}^{\sigma\rho} - \partial_\nu\partial_\rho\overline{h}^{\rho}_{\mu} - \partial_\mu\partial_\rho\overline{h}^{\rho}_{\nu} = -\frac{16\pi G}{c^4}T_{\mu\nu}, \tag{1.13}$$

where $\Box = \partial_\sigma\partial^\sigma = -\frac{1}{c^2}\frac{\partial^2}{\partial t^2} + \frac{\partial^2}{\partial x^2} + \frac{\partial^2}{\partial y^2} + \frac{\partial^2}{\partial z^2}$. This equation can be drastically simplified by choosing the right gauge for $\overline{h}$: by setting

$$\partial_\mu\overline{h'}^{\mu\nu} = \partial_\mu(h_{\mu\nu} - \partial_\mu\xi_\nu - \partial_\nu\xi_\mu) = 0, \tag{1.14}$$

where the term ξ is given for any infinitesimal transformation $x'^\mu = x^\mu + \xi^\mu(x)$; it can be shown that Einstein's equations become

$$\Box h^{TT}_{\mu\nu} = -\frac{16\pi G}{c^4}T_{\mu\nu}, \tag{1.15}$$

whit $h^{TT} \equiv \overline{h'}$.

1.3.1 Vacuum solution

In vacuum we have $T_{\mu\nu} = 0$, and the linearized Einstein equations lead to

$$\Box h^{TT}_{\mu\nu} = 0. \tag{1.16}$$

This equation has the form of a wave equation and represents the *gravitational wave equation*. It has a plane wave solution: $h^{TT}_{\mu\nu} = A_{\mu\nu}e^{ik_\sigma x^\sigma}$, where $\vec{k}$ is the GW's wave vector. Putting this equation in the latter we can see that the amplitude of the wave propagating along the z-axis is:

$$A_{\mu\nu} = h_+ \begin{pmatrix} 0 & 0 & 0 & 0 \\ 0 & 1 & 0 & 0 \\ 0 & 0 & -1 & 0 \\ 0 & 0 & 0 & 0 \end{pmatrix} + h_\times \begin{pmatrix} 0 & 0 & 0 & 0 \\ 0 & 0 & 1 & 0 \\ 0 & 1 & 0 & 0 \\ 0 & 0 & 0 & 0 \end{pmatrix}. \tag{1.17}$$

GWs have then two polarizations: + and ×, with respective amplitude $h_{+,\times}$. They act on a set of particles by "squeezing" spacetime with a sine-like function. A representation of this is shown in fig.1.1 and fig.1.2.

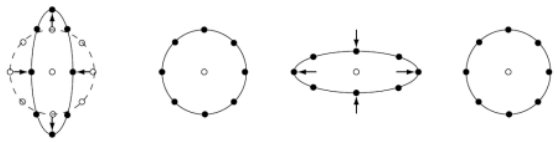

Figure 1.1: + polarization. The ring is made of test masses and lies in the xy-plane. The wave is propagating along the z direction ($\vec{k}//z$), perpendicular to the ring.

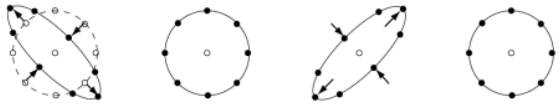

Figure 1.2: $\times$ polarization. The ring is made of test masses and lies in the xy-plane. The wave is propagating along the z direction ($\vec{k}//z$), perpendicular to the ring.

We have seen how gravitational waves act on spacetime: they produce an oscillation on the perturbative term of the metric tensor. Moreover, we have studied how spacetime and gravity are seen after Einstein's General Relativity. The last thing left to see is how to detect GWs.

1.3.2 The detection of Gravitational Waves

Modern experiments, such as LIGO and VIRGO, detect GWs using interferometers. For example, the scheme of the VIRGO detector is shown in Fig.1.3 [9]. From the laser, a beam of photons is sent

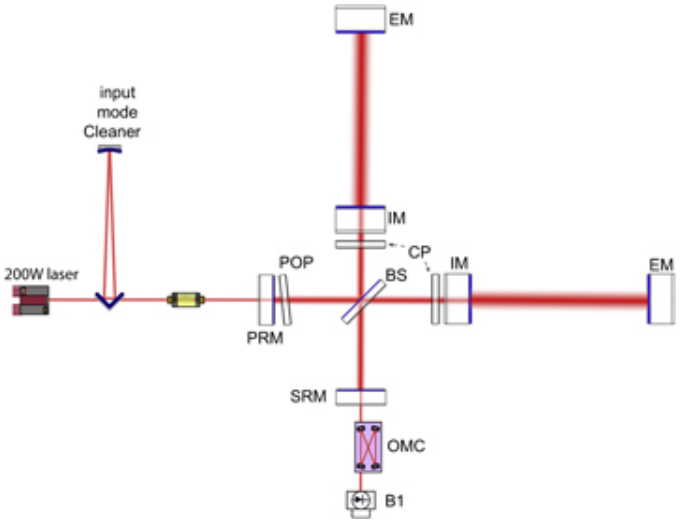

Figure 1.3: A scheme of the aVIRGO detector. The laser beam starts from its source on the left. In the splitter (in the center) it is splitted in two perpendicular beams. After their passage in the Fabry-Perot Cavity, they come back to the splitter. They are rejoined in the final beam, which travels to the photodiodes. In the photodiodes the beam's intensity is measured, and so the phase difference of the light in the two arms.

to a beamsplitter and it splits in two perpendicular beams, each one travelling in a straight arm of length $L_{x,y}$ (assuming one arm is along the x-direction and the other along the y-direction). They are reflected back to the beamsplitter and here they are recombined[2] and sent to photodiodes. When a GW passes, the propagation of the light in the arms is modified and the two perpendicular beames acquire different phase. In the photodiode the intensity of the reconstructed beam is measured, and therefore the total phase difference. However, in order to quantify this phase displacement we should pay attention to which frame to use. In all the previous calculations I used the TT gauge frame, and hence I derived the GW equation (1.16). In this frame the coordinates of free falling masses do not change, even when a GW is passing. Thus, in the TT gauge description, the coordinates of the mirrors and of the beam-splitter, which are free falling, are not affected by the passage of the wave. The physical effect of the GW is manifested in the fact that it affects the propagation of light between these fixed points.

The phase displacement is

$$\Delta\phi = \omega_{em}(\Delta t_y - \Delta t_x) - k_{em}(\Delta L_y - \Delta L_x), \tag{1.18}$$

[2]The total distance travelled seems to be 2L. Actually, Fabry-Perot cavities (in which photons bounces several times between two mirrors) are used. This drastically increase the actual distance travelled.

where ω_{em}, k_{em} are relative to the light and $\Delta t_{x,y}$ is the time interval in which the beam travels the arms:

$$\Delta t_y = \frac{2L_y}{c} - \frac{L_y}{c}\frac{\sin\left(\omega_{gr}L_y/c\right)}{\omega_{gr}L_y/c}h_+\left(t_0 + \frac{L_y}{c}\right), \tag{1.19}$$

$h_+(t) \equiv h_+\cos(\omega_{gr}t)$ is the perturbation along the +-direction caused by the GW. $\Delta L_{x,y}$ is the difference in the length of each arms that a GW may cause. However, from the properties of the TT gauge follows that the ΔL term does not contribute to the phase because the coordinate length of the arms remains the same, hence the spatial contribution to the phase does too. Indeed the actual phase difference is

$$\Delta\phi = \omega_{em}(\Delta t_y - \Delta t_x). \tag{1.20}$$

The same result, but in an approximation form, can be found if one works in the proper detector frame (defined by rods and giroscopes) and makes use of the geodetic deviation equation: here the effect of the GW is a "displacement" of the test masses from their original position. In fact, as stated by M.Maggiore in Ref. [11]

> "In the TT gauge, the position of the mirrors is not affected by GWs, while the propagation of light between the mirrors is affected. In the proper detectors frame, the mirrors are affected by the GWs, while light propagation is not."

The full derivation for both frames and their comparison can be found in Ref. [11].

Studying the interference figure we can find $\Delta t_{x,y}$ and then the GW's waveform h_+.

Chapter 2

Memory Effect

I will now consider the GW originated from the merging of massive objects, for example two merging BHs. As shown in all the standard pictures of waveforms, the plot seems to start from zero, builds to some maximum, and then apparently decays back to zero after the passage of the wave. In term of spacetime: it starts oscillating from a flat Minkowskian manifold without perturbation, curves, and finally comes back to the flat state after the wave passage. For example, in the first merging of two black holes detected by the twin LIGO observatories the waveform plot is shown in Fig.2.1[1]:

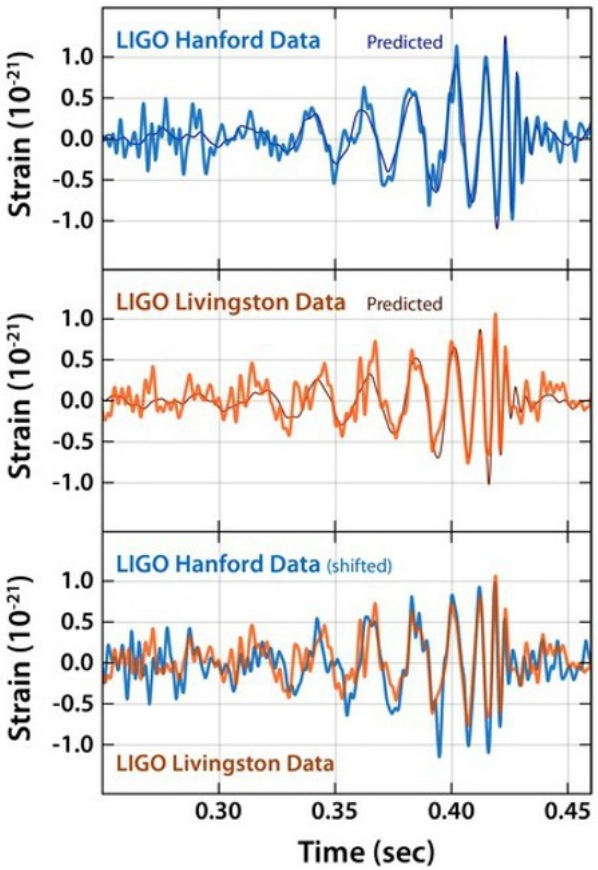

Figure 2.1: Experimental strain measured by the LIGO detectors in the GW150914 event. The irregular curves are the experimental data, the smoother ones are the predicted waveforms. In the last frame the data are overlapped in order to show that it is the same signal.

where the strain represents the fractional amount by which distances are distorted. As we can read

[1]Pictures download from `https://www.ligo.caltech.edu/image/ligo20160211a`

from the graphs, after the wave burst the plot comes back to zero.

In reality this statement is not true: in fact, the works made by Braginsky et Thorne [3], Blanchet et Darmour [5] and Christodoulou [6] suggest that a new effect is predicted by the theory of general relativity: the *Memory Effect*.

When a GW passes through a detector it causes a momentary deformation (in its proper frame) given from $\delta l_j = \frac{1}{2} h^{TT}_{jk} l^k$ (where l^k is the initial distance), but eventually the detector should return to its initial state. Instead, if we consider the memory effect in an idealized detector (so the masses are really freely falling), it causes a permanent deformation, a difference in their relative position, leaving a "memory" of its passage. Moreover, the memory of a gravitational wave burst not only is the permanent displacement of free test masses, but it's the permanent change in the field h^{TT}_{jk}. In other words: spacetime remains perturbed.

In more general terms, not only the merging of black holes generates a memory effect, but all GW sources possess some form of memory, and this effect can be expressed as

$$\Delta h^{mem}_{+,x} = \lim_{t \to +\infty} h_{+,x}(t) - \lim_{t \to -\infty} h_{+,x}(t) \neq 0, \tag{2.1}$$

where, with obvious notation, the first term (limit to $+\infty$) is the final state after the GW burst, and the second one (limit to $-\infty$) is the initial state before the GW burst. So the actual plot we should expect from a GW with memory is something more similar to the one in fig.2.2[2]. It can be clearly seen that the perturbation h doesn't come back to zero after the wave has ended.

The actual effect of the memory of test masses can be seen in fig.2.3.

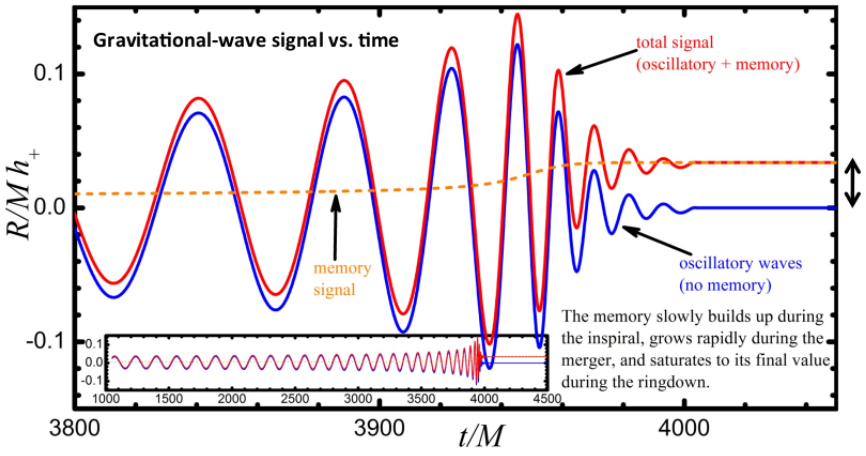

Figure 2.2: Memory effect on a waveform plot. The blue waveform does not have memory, the red one does. The memory signal is the dotted orange line. Note that the memory builds up during the whole merging, with a higher speed during the wave's frequency peak.

Unfortunately, the residual displacement is very small compared to the oscillatory part of the GW that we can measure. This explains why it has not been observed yet; but, as I will show in the last chapter, experimental prospects for this can leave us optimistic.

This was a qualitative overview of this new effect predicted by general relativity. Studying the possible sources of the memory it is found that this effect is actually divided in two contributions: the *linear memory* and the *non-linear memory*.

[2] `http://www.phy.olemiss.edu/StronGBaD/talks/Favata.pdf`

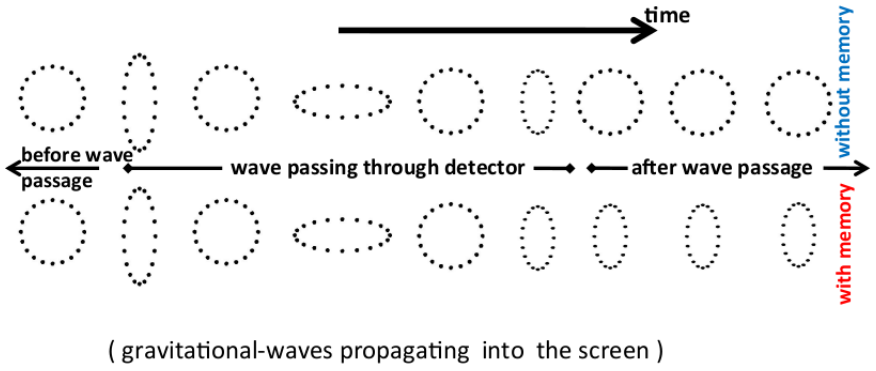

Figure 2.3: Qualitative effect of the memory on test masses and spacetime. Without the memory, after the wave passage, the test masses come back to a circumference (the same as before the wave passage). With the memory the masses do not come back to a circumference, but they remain perturbed.

2.1 Linear effect

The linear memory effect arises from a non-oscillatory motion of a source or in systems with unbound components: binary on hyperbolic orbit, matter ejected from a supernova or gamma-ray burst jets.

It originates from considering the linearized version of Einstein's equations if we assume we are in the weak field approximation, for examples when we are so far from the source that the GW amplitude is very small. If we consider the linearized, harmonic Einstein field equations for the space-space piece h^{TT}_{jk} (the j,k indexes runs on the cartesian coordinates x,y,z), and compute them using the stress-energy tensor for N gravitationally unbound masses, labeled by the index A={1,2,...,N} and projecting to transverse-traceless (TT) gauge can be found [3], [12]:

$$h^{mem}_{jk} = \Delta \sum_{A=1}^{N} \frac{4M_A}{R\sqrt{1-v_A^2}} \left[\frac{v_A^j v_A^k}{1 - v_A \cos\theta_A} \right], \tag{2.2}$$

where $h^{mem}_{jk} \equiv \Delta h^{TT}_{jk}$. From now on the TT gauge apex will be omitted for a lighter writing. In the equation above I assumed $G = c = 1$, the full version of eq.(2.2) is

$$h^{mem}_{jk} = \frac{G}{c^2} \Delta \sum_{A=1}^{N} \frac{4M_A}{R\sqrt{c^2-v_A^2}} \left[\frac{v_A^j v_A^k}{c - v_A \cos\theta_A} \right]. \tag{2.3}$$

The Δ on the right-hand side of the equation means that the difference between the final value of the summation and the initial value has to be taken (as in (2.1)). M_A are the masses of the bodies, R is the distance of the source from the observer at the moment of the emission measured on the observer frame, $\vec{v}_A$ is the velocity of the A-body and θ_A is the angle between v^j_A and the direction from the source to the observer. As we can see this formula depends only from the properties of the sources and the relative position with the observer; no interactions are taken in consideration. The only constraint is that the masses must move freely. Sources like the collision of two or more masses (if gravitationally free) or an explosion of an initial mass into several free masses are both good candidates that can be computed in the previous formula.

If the gravitationally-free condition is satisfied, the physical interpretation is clear: the memory in the metric field is due to the change in the initial and final values of the masses and velocities, or in general the linear momentum, of the system components. The sources of the field change, so does spacetime. As written by V.B.Braginsky and K.S.Thorne in Ref. [3]:

> "[...] so long as the source is not at a cosmologically large distance, the permanent change in the gravitational-wave field (the burst's memory) δh^{TT}_{jk} is equal to the 'transverse, traceless (TT) part' of the time-independent, Coulomb-type, $1/r$ field of the final system minus that of the initial system."

It becomes even clearer if we rewrite the (2.2) as

$$h^{mem}_{jk} = \Delta\left(\sum_{A=1}^{N} \frac{4P^A_j P^A_i}{\vec{k}\cdot\vec{P^A}}\right), \tag{2.4}$$

where $\vec{P^A}$ is the 4-momentum of mass A, P^A_i is one of its spatial components measured in the observer frame and $\vec{k}$ is the past-directed null 4-vector from observer to source. Now it is clear that physically what have to change are the linear momenta of the constituent bodies.

Mathematically, this descends from the analytical form of the $h_{\mu\nu}$ tensor. As seen in the first chapter, Einstein Field Equations (EFE), in the general case, take the form:

$$\Box h_{\mu\nu} = -\frac{16\pi G}{c^4} T_{\mu\nu}. \tag{2.5}$$

All the information on the masses we are considering, their velocity and distribution are contained in the stress-energy tensor: $T_{\mu\nu} = \rho_0 u_\mu u_\nu$ (where $u_\mu = (c\gamma, \gamma\vec{p})$). Solving the differential, non-homogeneous, coupled field equations, is not easy. Luckily the analytical solution is known:

$$h_{\mu\nu}(ct, \vec{x}) = \frac{4G}{c^4}\int \frac{T_{\mu\nu}(ct - |\vec{x}-\vec{y}|, \vec{y})}{|\vec{x}-\vec{y}|} d^3y, \tag{2.6}$$

$\vec{x}$ is the distance at which I compute the gravitational wave, $\vec{y}$ is a point running on the source and $ct - |\vec{x}-\vec{y}|$ is the retarded time and is denoted with ct_{ret}. Let us now suppose being in a long distance approximation: $R \gg D$ (D is the extension of the body we are considering, R is the distance between the observer and the source) and $|\vec{x}-\vec{y}| \approx R$. The spatial components of the equation are:

$$h_{ij} = \frac{4G}{c^4 R}\int T_{ij}(ct_{ret}, \vec{y}) d^3y = \frac{2G}{c^6 R}\frac{d^2}{dt^2_{ret}}\left[\int T_{00} y_i y_j d^3y\right]. \tag{2.7}$$

The quantity between square brackets is called *quadrupole moment tensor*:

$$I_{ij} \equiv \int T_{00} y_i y_j d^3y. \tag{2.8}$$

Remembering that the 00 component of the stress-energy tensor is the energy density, and finally writing the solution:

$$h_{ij} = \frac{2G}{c^6 R}\frac{d^2 I_{ij}}{dt^2_{ret}}, \tag{2.9}$$

all the previous considerations on the physical aspects of the linear effect are clear: when the masses collide, explode or eject other masses, we have a linear memory if the quadrupole moment changes. This is because the energy density changes, and so does the quadrupole moment. Yet, this is not enough: the quadrupole moment has to change "accelerating" and not at a "constant speed", in fact what has to be non-zero is its second time derivate and not the quadrupole moment itself, nor its first time derivate.

2.2 Non-linear effect

As we saw, the linear effect arises from the linearization of Einstein's equations. This is a legit approximation if we think that GW sources are at enormous distance from Earth, indeed the amplitude of the waves is very small. The weak field approximation seems sufficient then.

However, as shown separately by Christodoulou and L.Blanchet & T.Damour, there is a *non-linear effect* (also known as Christodoulou effect) [5], [6]. This effect arises from the full nonlinear equations, and it's sourced by the cumulative stress-energy of the radiated GWs. In the same way a difference in the source's stress-energy tensor sources GWs and a linear memory, the stress-energy tensor carried by the waves generates a sort of "second order" memory. This non-linear effect is purely due to the EFE non-linearity and it isn't an approximation.

Given that it isn't a first order effect like the linear one, it could be expected to be orders of magnitude smaller. Actually, for a binary coalescence, the nonlinear memory is of the same order of magnitude as the maximal amplitude of the dynamical part of the burst. This forces us to take it into account when computing the memory left after a GW.

GW's stress-energy tensor interpretation

The analytical expression for the non-linear memory is [2]:

$$h_{jk}^{mem} = \frac{4G}{Rc^4}\int_{-\infty}^{T_R} dt' \left[\int \frac{dE^{gw}}{dt' d\Omega'} \frac{n'_j n'_k}{(1-\mathbf{n}'\cdot\mathbf{N})} d\Omega'\right], \tag{2.10}$$

T_R is the retarded time, n_j is a unit radial vector, $\mathbf{N} = \mathbf{x}/r$ is the unit line-of-sight vector drawn from the observer at Earth to the source and $\frac{dE^{gw}}{dtd\Omega}$ is the GW energy flux. Both left and right side of the equation are computed in the TT gauge. The integrals are over the solid angle $d\Omega'$ surrounding the source and over the time dt'. The time integral gives the memory an hereditary nature: its amplitude depends on the entire past history of the source. Physically, the memory gets built up continuously over the duration of the burst. This is obvious if we think on how the previous formula was derived in [2]: the first GW carries a stress-energy distribution which, while it is emitted, generate other (second order) GWs. So this nonlinear contribution gets built up during the whole emission of the GW. The energy flux term arises from the complete EFE solution

$$\Box \overline{h}_{\alpha\beta} = -16\pi\tau_{\alpha\beta}, \tag{2.11}$$

where $\tau_{\alpha\beta}$ is the *effective stress-energy tensor*, that depends on the matter stress-energy tensor $T^{\alpha\beta}$, the Landau-Lifshitz pseudotensor $t_{LL}^{\alpha\beta}$ and other terms quadratic in $\overline{h^{\alpha\beta}}$. In $t_{LL}^{\alpha\beta}$ there is a term proportional to the stress-energy tensor for GWs:

$$T_{jk}^{gw} = \frac{1}{R^2}\frac{dE^{gw}}{dtd\Omega} n_j n_k. \tag{2.12}$$

It can be shown that the GW energy flux is:

$$\frac{dE^{gw}}{dtd\Omega} = \frac{R^2 c^3}{16\pi G}(\dot{h}_+^2 + \dot{h}_\times^2), \tag{2.13}$$

where $\dot{(\,)} \equiv d/dt$, so $\dot{h_+}$ and $\dot{h_\times}$ are the speed at which the two polarizations of the wave oscillate. Those contributions enter in the integral (2.10) and indeed in the non-linear memory. This justifies our initial interpretation of this memory as generated by GWs, and not by changes in the source as in the linear one.

In fact, thinking in terms of quadrupole momentum like for the linear memory, we can express the non linearity as a correction to the multipoles. Putting $T_{\alpha\beta}^{gw} \propto dE^{gw}/dtd\Omega \sim O(h^2)$ in the (2.7) we find a correction term in the quadrupole momentum

$$\ddot{I}_{jk} \to \ddot{I}_{jk} + U_{jk}^{gw}(T_{\alpha\beta}^{gw}) \to \ddot{I}_{jk} + U_{jk}^{gw}\left(\frac{dE^{gw}}{dtd\Omega}\right) \tag{2.14}$$

that can eventually be computed in the linear memory (2.9) as an unique term.

In other words: the non-linear memory can be seen as a sort of linear memory generated by gravitational waves and not directly by an astrophysical source like BH-BH coalescence, gravitational scattering, neutrinos burst, etc. Nevertheless, one should remember that this interpretation is right only if we want to have a first idea of what is going on. The origins of the linear and non-linear memory are drastically different: the first one arises from the EFE linear approximation, the latter from the full non-linear equations (Christodoulou in Ref. [6] made the whole calculation from the full version). Also the conditions on the source are very different: in order to have a linear memory the objects before and after the collision, scattering or burst, have to be gravitationally independent. Clearly this condition does not hold when considering BH-BH or NS-NS coalescence.

From the reasonings above it follows that:

- memory piece scales like the radiated energy: $\Delta h^{(mem)} \sim \Delta E^{gw}/R$;
- nonlinear memory is present in all GW sources;
- the effect is hereditary (as seen with the time-integral).

Gravitons interpretation

Another interesting interpretation was proposed by K.Thorne in [12]. He stated that the nonlinear memory is included in the general expression (2.2) of the memory. In fact, it can be seen as the contribution to (2.2) from the gravitational-wave burst's gravitons. Let us consider each graviton as a particle with energy E_A (measured in the detector's rest frame) and speed $v_A = c$. If we take the linear memory equation (c=G=1) and regard every single graviton as an individual particle, we have to include them only in the final summation, because they are ejected with the burst, so they don't appear before their emission. Starting from the linear memory

$$h^{mem}_{jk} = \Delta \sum_{A=1}^{N} \frac{4M_A}{R\sqrt{1-v_A^2}} \left[\frac{v_A^j v_A^k}{1 - v_A \cos\theta_A} \right] \tag{2.15}$$

and substituting

$$\begin{aligned} v_A^j &\to c n_A^j \\ E_A &\to \frac{M_A c^2}{\sqrt{1-v_A^2}}, \end{aligned} \tag{2.16}$$

we obtain

$$h^{mem}_{jk} = \Delta \sum_{A=1}^{N} \frac{4E_A}{R} \left[\frac{n_A^j n_A^k}{1 - \mathbf{n}_A \cdot \mathbf{N}} \right]. \tag{2.17}$$

We can see that the term between square brakets is identical to the one in the (2.10) equation. Gravitons, like GW, are emitted in all directions, so we can now consider the graviton's energy distribution $\frac{dE}{d\Omega}$ and, integrating over the solid angle Ω, we find

$$h^{mem}_{jk} = \frac{4}{R} \int \frac{dE}{d\Omega} \left[\frac{n^j n^k}{1 - \cos\theta} \right] d\Omega, \tag{2.18}$$

where θ is the angle between n^j and the detector. This is the linear contribution given from gravitons emitted in all directions. However, this last integral is calculated at a fixed time, but we have seen that the non-linear memory is an hereditary effect (it depends by the whole source's history). Gravitons, then, have to be emitted throughout all the process: this suggests we have to integrate (2.18) also over time. Eventually we get

$$h^{mem}_{jk} = \frac{4}{R} \int_{-\infty}^{T_R} dt \left[\int \frac{dE}{dt d\Omega} \frac{n_j n_k}{(1 - \mathbf{n}' \cdot \mathbf{N})} d\Omega \right], \tag{2.19}$$

which is identical to the first equation (2.10) deducted by the full nonlinear EFE (here we use G=c=1 natural units) by Christodoulou.

The gravitons interpretation also holds up with the "waves of the wave" picture we described in the GW's stress-energy interpretation. In fact, as I said, the nonlinear memory can be seen as a sort of memory sourced by the waves generated by the initial GWs. It's a GW self-interaction. This is still valid with the particle point of view: because of EFE nonlinearity every graviton self-interacts with itself.

Regardless the clarity and elegance of this interpretation, one must remember that gravitons are still only a theoretical prediction. This prediction has strengthened in light of the latest GW observations (due to the quantum particle-wave dualism), but despite that, there is still no detection of gravitons up to the publication of this thesis (March the 25th, 2019). Only further experiments will prove or disprove it.

2.3 Computing the memory in BHs coalescence

I will now show how the memory can be practically computed in order to make experimental predictions. First of all, one should consider which memory we have in coalescence events. Given that the two bodies (BHs or NSs) are gravitationally bound there's only nonlinear memory. However, computing the full summation (2.2) (in case of a linear memory event) or integral (2.10) is anything but easy. It will only be time and resources consuming. The best way to proceed is to use numerical relativity and some approximations.

Thorne showed that the formula (2.10) can be written as

$$h_{mem}(t) = \frac{2}{R}\int_{-\infty}^{t} dt' \int d\Omega' \frac{d^2E}{dt' d\Omega'}(1+\cos\theta')e^{2i\phi'} \tag{2.20}$$

if we choose an arbitrary x directions in the detector plane, then ϕ is the angle in that plane of the source respect to the x-axes. Expressing the energy flux in terms on spherical harmonics it has been found [13]:

$$h_{mem}(t) = \Phi(\iota)\frac{R}{4\pi c}\int_{-\infty}^{t} dt' \dot{h}_+^2, \tag{2.21}$$

where r is the observer-binary distance expressed in meters (throughout all the thesis I work in Mpc, so a conversion has to be made), $\dot{h}_+$ is the speed of the h_+ oscillation (the wave is supposed to be polarized only in the + polarization) and c is the speed of light. The $\Phi(\iota)$ factor modulates the amplitude of the memory depending from the angle ι between the angular momentum of the binary and the observer-source direction

$$\Phi(\iota) = \sin^2\iota\left(1 - \frac{\sin^2\iota}{18}\right). \tag{2.22}$$

Clearly the maximum memory amplitude is obtained for edge-on binary systems ($\iota = \pi/2$), in contrast to the primary oscillatory wave which is strongest from face-on binaries ($\iota = 0$) in which, indeed, the memory effect is not present ($\Phi = 0$).

To compute the memory I used the PyCBC Python package [14] to generate the waveform of my event, then, with a few added lines for printing in an output file the data, I computed the integral (2.21), obtaining the time domain memory function. The simulation algorithm used for the GW waveform is SEOBNRv2.

From the linear dependency in the distance in (2.21), it may seems that the farther I am from the merging the higher the memory amplitude is. However, the GW's amplitude decreases with the distance, so also the memory is expected to do so. Indeed, even in the theoretical formula (2.20) the amplitude of the memory goes like $1/R$, so it decreases with the distance. In fact, there is another

distance dependency inside the integral, in the computation of $\dot{h}_+^2$. This resolves the amplitude-distance problem: the final amplitude goes approximately like $\sim 1/R$, so it eventually decreases with the distance. In the table below are shown the expected memories from different mass-distance binaries. Masses are in solar masses unit, distances are in Mpc and in every binary the BHs have the same mass. As can be seen, the memory decreases with the distance and increases with the total mass of the binary.

		Distance [Mpc]		
		1	100	1000
$M_{tot}[M_\odot]$	10	6.40×10^{-21}	6.40×10^{-23}	6.40×10^{-24}
	100	7.39×10^{-20}	7.39×10^{-22}	7.39×10^{-23}
	1000	6.65×10^{-19}	6.65×10^{-21}	6.65×10^{-22}

The memory also depends on the BHs's masses ratio and not only on the total mass of the binary. I calculated the memory for BHs binaries with $d = 100$Mpc, $s = 0$ but different mass-ratio

$$\eta \equiv M_{min}/M_{max}.$$

From the results in the table below it can be seen that the amplitude of the memory increases with η tending to 1, at which we have maximum amplitude.

M_1/M_2	η	$h_{mem}[\times 10^{-22}]$
50/50	1	7.39
40/60	0.67	6.80
30/70	0.43	4.99
20/80	0.25	2.90
10/90	0.11	1.02

This dependency is indirect: in the (2.21) the total mass or masses enter only in the integrand and not directly in the formula. Indeed, variations in the memory from masses variations are due to differences in the waveform. The different waveforms for two mergings with different η can be seen in fig.2.4.

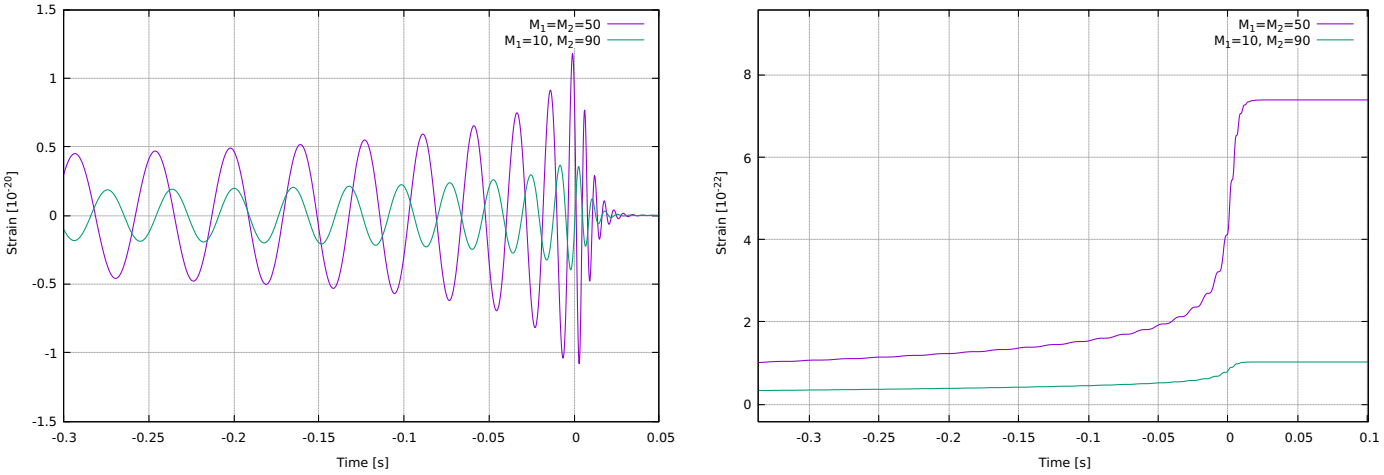

Figure 2.4: Waveform (left plot) and memory (right plot) comparison for two BHs mergings: one with $M_1 = M_2 = 50M_\odot$ and the second with $M_1 = 10M_\odot$ and $M_2 = 90M_\odot$. Both are at d=100Mpc. Despite having the same distance and total mass, these two binaries generate different memories due to different GW waveforms. The time scale is set to have the BHs collision at $t = 0$s.

2.3.1 GW150914 Memory

For a GW150914-like event the parameters I used in the code are:

- $m_1 = 36M_\odot$, $m_2 = 29M_\odot$;
- spin = 0;
- distance = 420 Mpc;
- dt = 0.00025 s;
- f_lower = 7.5 Hz.

dt is the time discretization between two data and f_lower is the lower frequency at which the simulation starts. The lower frequency is outside the LIGO band so it wouldn't be detected, but I chose a low value in order to obtain more data and approximate better the time integral (which should start from $t = -\infty$). The waveform and the memory obtained are shown in Fig.2.5.

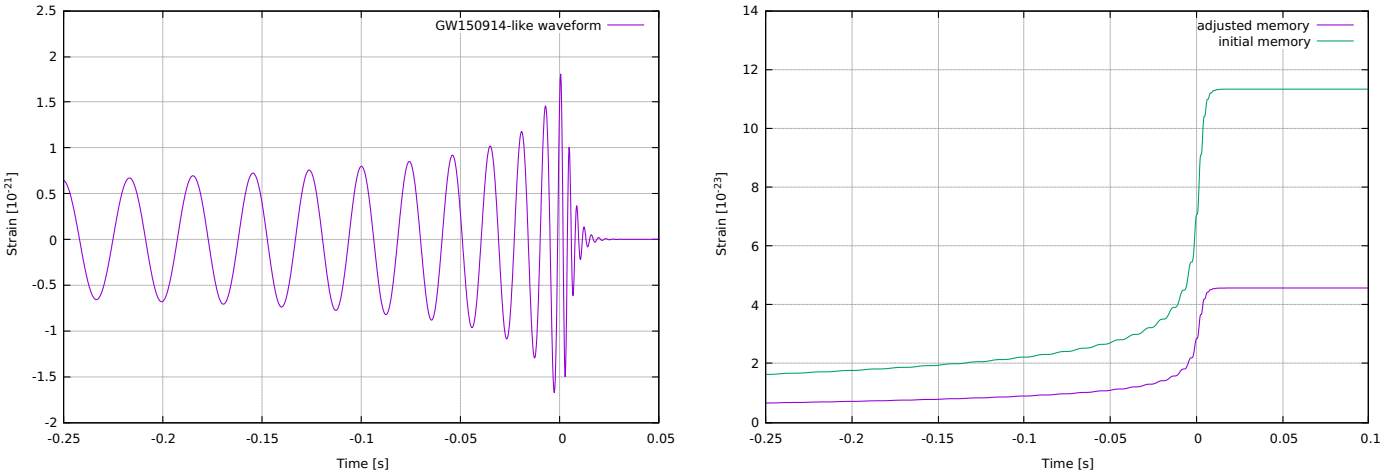

Figure 2.5: In the left frame is shown the waveform of a GW150914-like event, with the parameters discussed above. The right plot is its memory. The green memory is obtained by the calculation of (2.21). Because of the differences in the parameters and algorithm, and the approximations in the (2.21) the actual memory is the adjusted (purple) curve.

The memory has to be adjusted by a factor $\Phi(140°) \approx 0.4037$ because the original memory calculated with Eq.(2.21) is an overestimate. This comes from different reasons: a difference in the binary parameters (masses, distance...), the algorithm used and the derivation of Eq.(2.21) itself. For computing a GW's waveform different algorithm can be used: MWM, SEOBNRv2, IMRPhenomC etc... LTLBC in [15] used the MWM approximation, instead I used the SEOBNRv2 algorithm. Hence, the waveforms are slightly different and, as a matter of fact, the amplitude of the memory is slightly different too. However, input parameters or the algorithm for the waveform can be changed without particular problems. The main reason for the adjusting factor lies on the derivation of Eq.(2.21): Johnson et all. in Ref. [13] derived their equation as an "easy to use and computationally cheap" alternative to a more advanced numerical relativity derivation, i.e. the derivation used in Ref. [15]. Computation of the nonlinear memory from numerical waveforms has proved difficult, instead a computation with Eq.(2.21) is way easier, time saving and leads to a pretty accurate result. The price to pay is a slightly difference in the amplitude of the memory waveform obtained, which can be easily resolved with a manual adjustment. To match the amplitude obtained from Eq.(2.21) with the amplitude obtained in Ref. [15] and other works, the factor required is equivalent to consider the binary with an inclination factor of $\Phi(140°)$ introduced above. The full discussion can be found in [13]. Note that in the previous subsections I omitted this factor because all I did were qualitative calculations. For more accurate and quantitative estimations of the memories you should remember to adjust them.

Finally, the full waveform with memory is shown in Fig.2.6.

From those graphics we can see some interesting things:

- the memory builds up during the whole bursts, as suggested by the time integral in (2.10);

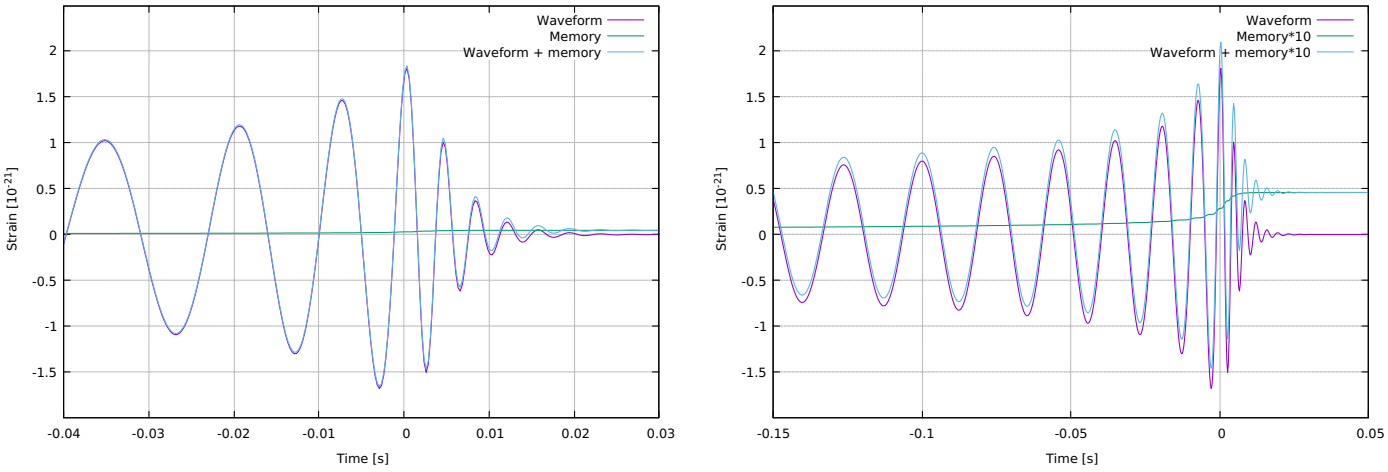

Figure 2.6: In the left frame is shown the total waveform (with the memory) for a GW150914-like event. In the right frame the memory is magnified by a factor 10 to better show its built up during the merger and its effect on the waveform

- the memory has a sort of "wiggliness": it isn't smooth as one would expect. This is due to the fact that in the (2.21) integral there should be a time average $\left\langle \dot{h_+}^2 \right\rangle$. Since we are integrating over the entire history of the source, the average has been dropped (see [13] for more details).

The amplitude of the memory we should expect is in the order of

$$h_{mem} \approx 10^{-23}, \tag{2.23}$$

so two orders of magnitude lower than the maximum amplitude of the wave. This shows why its detection is so difficult.

Expected SNR in the aVIRGO O3 run

Using the expected noise data for the aVIRGO detector in its O3 run (starting on 1st April 2019) [17], I calculated its expected signal to noise ratio (SNR) for the memory of a GW150914-like event. The SNR integral I should have computed is [13]:

$$\rho^2 = 4 \int_0^\infty \frac{|\tilde{h}(f)|^2}{S_n(f)} df, \tag{2.24}$$

where ρ is the SNR, $\tilde{h}(f)$ is the memory signal in the frequency domain obtained from eq.(2.21) (in fig.2.5) and $S_n(f)$ is the one sided noise power spectral density (PSD).

Instead of computing the integral, I decided to use Mathematica and compute a discrete summation. This choice is due to the fact that the memory signal is sampled in time and I do not have its analytical form. My memory waveform is sampled with a time discretization of $dt = 0.00025$s and for a time window of 8s, so I have 32000 samples. Applying a Fast Fourier Transform (FFT) on the memory, I obtain a memory signal in the frequency domain with 16000 samplings (I only take positive frequencies) and discretization of $df = 0.125$Hz. In order to have a matching PSD I had to fit the given noise data and then sample the analytical function (with the Map[ ] operator) over a list of frequencies from 0.125Hz to 2kHz, with a discretization of $df = 0.125$Hz. The analytical equation for the expected aVIRGO noise in the O3 run I found is

$$S_h(f) = S_0 \left((7.3x)^{-5} + 0.125x^{-1} + x^2 \right), \tag{2.25}$$

with $S_0 = 13.2 \times 10^{-47}\text{Hz}^{-1}$ and $x = f/(258\text{Hz})$. The fitting function and the expected noise can be seen in Fig.2.7

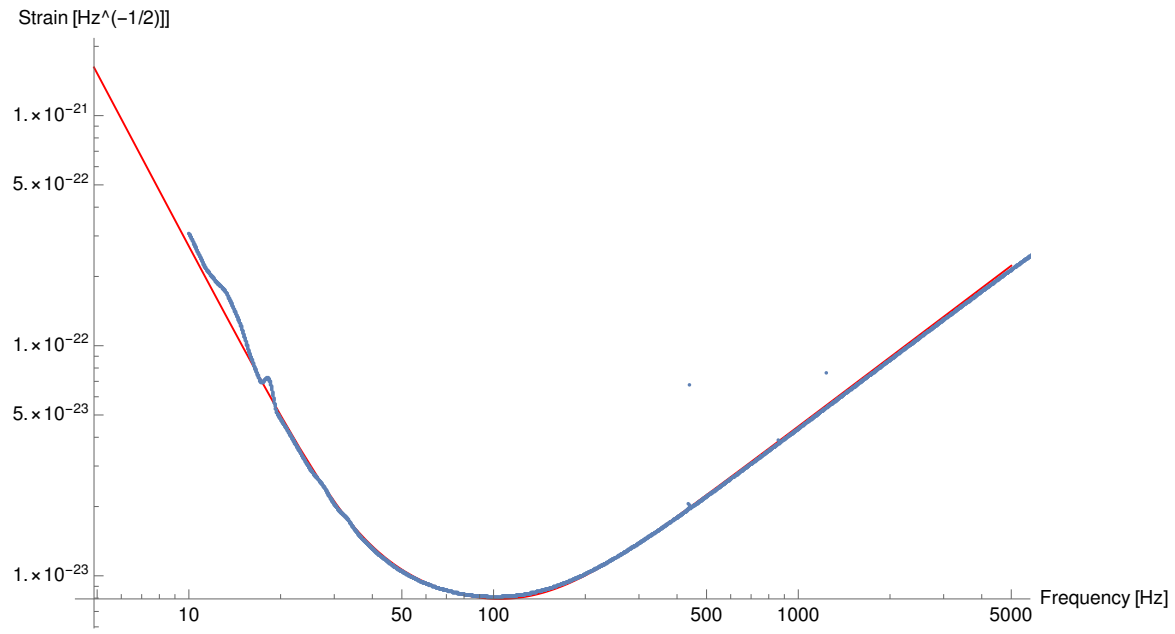

Figure 2.7: Comparison between the expected aVIRGO noise (blue points) and the fitting function given by Eq.(2.25) (red curve). The fit is a good approximation, with a small deviation in the [10-20] Hz interval. Given the very small residuals of the fit, this deviation does not affect my results.

Once I computed the FFT for the memory signal and adjusted its normalization coefficients, the final summation obtained was

$$\rho = \left[\sum_{i=0}^{N_s} \frac{|\tilde{h}[i]|^2}{(0.125 * S_n[i])^2} \right]^{1/2}, \tag{2.26}$$

where the i index runs in the lists of the FFT of the memory signal and of the PSD. N_s is the number of the FFT samples (16000). The SNR obtained is:

$$\rho = 0.263, \tag{2.27}$$

which is too much small to contribute significantly to the detection. Consequently, for a single GW150914-like event in the aLIGO O3 run, the memory can not be detected.

A.D.Johnson et all. in Ref. [13] calculated an SNR for a GW150914-like event for aVIRGO of $\rho = 0.238$, which agrees with mine. They also calculated the SNR for two aLIGO detectors at design sensitivity of $\rho = 0.45$ [13], while Lasky et all. in Ref. [15] found $\rho = 0.42$. These values are higher then mine because aLIGO has two interferometers, so the final SNR is the summation of two single-detector SNR. However, they are still to low to claim detection with a single event.

Chapter 3

Experimental perspectives

This chapter will deal with (some of) the experimental possibilities to detect the memory. This is a fundamental aspect not only in the Memory Effect discussion, but also in the physics of gravitation. Without a possible detection previous discussions would remain in the realm of mathematics.

3.1 Direct Observation

Assuming a SNR threshold for detection as SNR=3, a single event detection is highly improbable as shown before. However, as shown in [15], a better strategy relies on the coherent summation of an ensemble of subthreshold signals. A coherent summation is requested because one should also consider the sign of the memory: if it isn't taken into account, the memory adds incoherently and cancels. However, to be determined, higher modes of the oscillatory signal have to be used. In fact, the h_{22} mode can't be used to determine the sign: it carries a degeneracy for the polarization angle Ψ and the phase at coalescence Φ_c. The h_{22} mode is invariant under a transformation $\Psi \to \Psi + \pi/2$ and $\Phi_c \to \Phi_c + \pi/2$, but the memory acquires a minus sign under said transformation:

$$h_{22}(\Psi, \Phi_c) = h_{22}(\Psi + \pi/2, \Phi_c + \pi/2), \qquad h_{mem}(\Psi, \Phi_c) = -h_{mem}(\Psi + \pi/2, \Phi_c + \pi/2).$$

From this degeneracy follows that higher modes are needed to calculate the memory sign.

For multiple events and detectors, the total SNR of the memory can be computed as the summation of all the SNR for each event in each detector:

$$\langle S/N_{tot} \rangle = \left(\sum_{i=1}^{N_e} \sum_{j=1}^{N_d} \langle S/N_{i,j} \rangle^2 \right)^{1/2}, \tag{3.1}$$

where N_e is the number of events and N_d is the number of detectors. Lasky et all. simulated an ensemble of events with the same masses and distance of the GW150914 binary, but with a random distribution of inclination, polarization and sky position. The plot of the total SNR is shown in Fig.3.1.

What is important to be noted from the plots is the number of events at which it intersects the horizontal line of our threshold $\mathrm{SNR}_{tot} = 3$ (dotted line). It is shown that a detection can be claimed after ~ 35 GW150914-like detection (@ aLIGO sensitivity), although it could happen with as few as ~ 20 events. Instead, if a threshold of $\mathrm{SNR}_{tot} = 5$ is taken (solid line) the number of binaries required to claim detection rises up to ~ 90, with a lower boundary of ~ 70.

Of course with the current aLIGO sensitivity and detection rate (~ 5 random events/year) this could take several years, but still it's not improbable. However, the detection rate is expected to increase with the 2019 upgrade, so a memory detection could happen earlier.

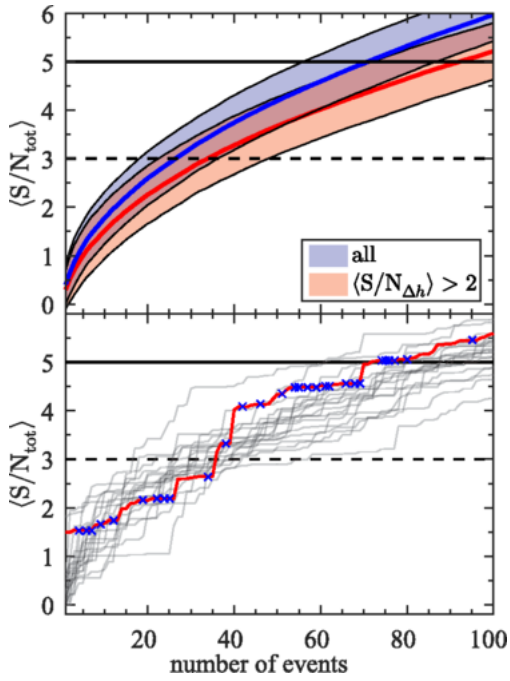

Figure 3.1: Evolution of the cumulative SNR_{tot} as a function of the number of BHs mergers from Ref. [15]. In the top panel the solid lines are the expectation value, their shaded regions are the one-sigma uncertainties. The blue one is the SNR_{tot} from all binaries, the red one is the SNR_{tot} without the events with undeterminated memory sign. In the bottom panel are shown 20 individual realizations of the red curve in the top panel. The highlighted line is just a particular one, the blue crosses are binaries with sign uncertainty.

3.2 Orphan Memory

The LIGO/Virgo interferometers have a detection band of $\sim 10 - 2000$ Hz. A GW with frequency outside that band will not be detected, but it could still leave a detectable memory. This memory will then be detected without parent signal: it is the so called *orphan memory*. As shown in Ref. [18], lower or higher frequency GW can be generated by an ensemble of different sources.

3.2.1 Low-frequency signal

Given that $f_{max} \sim 1/M$, a lower band signal can be a GW sourced by two supermassive BHs merging. In the GW150914 event the total mass of the system was $M_1 \sim 65 M_\odot$, and the maximum frequency was $f_1 \sim 250$ Hz. For a GW with frequency on the lowest band limit, $f_2 = 10$Hz, the mass should be:

$$M_1 f_1 = M_2 f_2 \Rightarrow M_2 = \frac{f_1}{f_2} M_1 = 1650 M_\odot.$$

For binaries with $M \gtrsim 1700 M_\odot$ we should expect an off-band GW that may source a detectable memory. However, the memory signal has most of its power at near-zero frequencies [19]. In fact, the memory has a rise time comparable to the whole GW's chirp but, in this chirp, the GW's signal oscillates several times, hence the GW maximum frequency is higher than the dominant frequencies in the power spectrum of the memory. As a matter of fact, for a supermassive BHs binary with a non detectable low frequency GW, the memory has a power peak at even lower frequencies, so it will not be detected. For example, in fig.3.2 are shown the GW's waveform and the memory for a BH-BH binary with $M_1 = M_2 = 1000 M_\odot$.

Excluding a macroscopic h_{mem}, sourced by a very close super-massive BHs merging, detectable also without interferometers, a lower-band GW memory is unlikely to be detected.

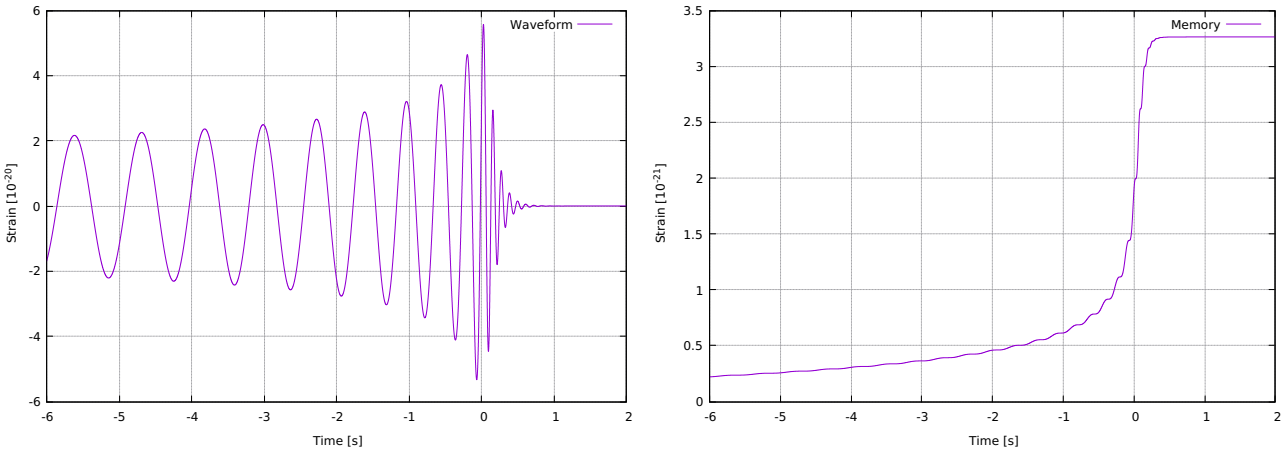

Figure 3.2: Waveform (left plot) and memory (right plot) sourced by a BHs merging, each BH has a mass $M = 1000M_{\odot}$ and the binary is at a distance of 420Mpc. The amplitude of the memory is not adjusted with the $\sim 40\%$ factor discussed in the previous chapter. The GW waveform has a frequency peak of approximately $\sim$ 8Hz and its memory has maximum power at even lower frequencies. Consequently, both of them would not be detected.

3.2.2 High-frequency signal

High-frequency GW can be generated by a number of astrophysical sources: black hole evaporation ($10^{10} - 10^{15}$ Hz), dark matter collapse in stars ($\sim$ 2 GHz) cosmic strings and Kaluza-Klein modes in higher-dimensional theories [18]. An orphan memory from an high-frequency GW can also be generated by BH-BH merging with particular masses and distance. As said above, the memory is a lower-frequency signal, so a BHs colescence with an off-band (in the high frequencies) GW can source an in-band memory. Because of this there is hope to have an in-band memory for an high-frequency signal.

For such signals an important help can be given by dedicated high-frequency detectors, such as Fermilab's "Holometer". In fact, as stated in [18]:

> "If high-frequency detectors observe a detection candidate, Advanced LIGO should look for a corresponding memory burst. A coincident memory burst could provide powerful confirmation that the high-frequency burst is of astrophysical origin. Similarly, if Advanced LIGO detects orphan memory, it may be worthwhile looking for coincident bursts in dedicated high-frequency detectors."

The combined use of both (along with other) detectors could then provide us with a powerful tools for both memory or other astrophysical phenomena detection. McNeill et. all. studied the curves of SNR=5 events for aLIGO and other high-frequency detectors (see [18] for the full list and nomenclature). The final plot can be seen in Fig.3.3.

From this comparison it can be seen that aLIGO should detect orphan memory before dedicated high-frequency detectors observe an astrophysical burst. So, it is more likely that aLIGO, with an orphan detection, suggests Holometer to look for a coincident burst. However, as stated by McNeill et all., a dedicated GW memory is desirable.

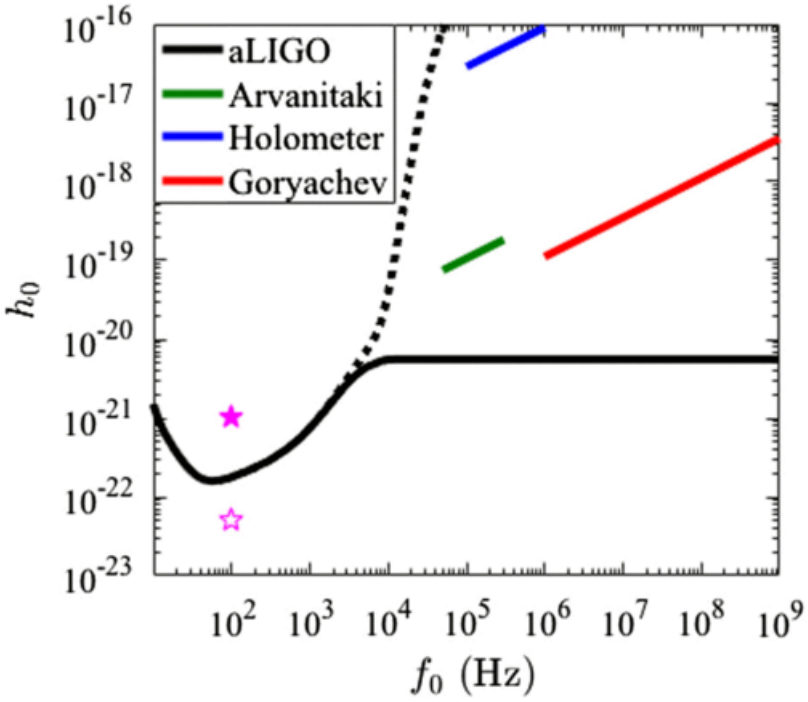

Figure 3.3: The black curves are the events, with amplitude h_0 and frequency f_0, with an aLIGO SNR=5. The solid one includes memory in the matched filter calculation. The blue curve is relative to Holometer. For comparison: the solid star indicates the maximum strain and frequency of GW150914 and the open one indicates its expected memory.

Conclusion

I have discussed the Memory Effect of gravitational waves and the differences in the linear and the non-linear contributions to the effect. The first is generated by the non oscillatory motion of the source, or the ejection of gravitationally unbounded masses. More in general, it is sourced by the change in the momentum of the system's center of mass. The second (Christodoulou effect) can be seen as a sort of "second wave" generated by the energy flux carried by the initial wave. I also shown that the non-linear memory can be interpreted as the linear memory generated by the emitted gravitons. Quantitatively, the linear memory can be calculated with

$$\Delta h^{lin}_{mem} = \frac{G}{c^2}\Delta \sum_{A=1}^{N} \frac{4M_A}{R\sqrt{c^2 - v_A^2}} \left[\frac{v_A^j v_A^k}{c - v_A \cos\theta_A} \right], \tag{3.2}$$

and, for the non-linear memory

$$\Delta h^{n-lin}_{mem} = \frac{4G}{Rc^4} \int_{-\infty}^{T_R} dt' \left[\int \frac{dE^{gw}}{dt' d\Omega'} \frac{n'_j n'_k}{(1 - \mathbf{n}' \cdot \mathbf{N})} d\Omega' \right], \tag{3.3}$$

remembering to take the TT gauge projection on both equations. I have shown how to compute approximately the memory sourced by a generic GW waveform as

$$h_{mem}(t) = \Phi(\iota) \frac{R}{4\pi c} \int_{-\infty}^{t} dt' \dot{h}_+^2. \tag{3.4}$$

For all the past GW events detected by LIGO and Virgo the memory amplitude was too small to be detectable over the interferometers noise. However, the method outlined in this thesis can be used to make experimental predictions on its detectability in future events. In particular, for BHs binaries the non-linear effect is the only possible memory that we can expect given the gravitational bound of the two objects. With the use of the PyCBC package, I have generated BHs mergings GW and computed their memory. The amplitude of the memory is maximum for same-mass binaries ($\eta = 1$) and decreases linearly with the distance. For a GW150914-like event we should expect a memory amplitude of

$$h_{mem} \sim 5 \times 10^{-23}.$$

However, for the aVIRGO detector in its O3 run the SNR of said memory is:

$$\rho = 0.263,$$

too low to be relevant for the detection. I have fitted the noise data and found its analytical form (Eq.(2.25)). A single detection is unlikely to happen in a near future. In light of the aLIGO/aVIRGO 2019 upgrade, a detection via an ensemble of events is more likely to happen in the future years. In fact, with a SNR threshold of 3 (5), 35 (90) GW150914-like events are required to claim detection; this may take years but it is not prohibitive. Moreover, high-frequency GW detectors paired with the interferometers can help to detect an Orphan Memory, a memory with an off-band GW, from different astrophysical and cosmological sources, not only BHs or NSs mergings.

Bibliography

[1] B.P.Abbott et al. (LIGO Scientific Collaboration and Virgo Collaboration) Phys.Rev.Lett. 116, 061102 (2016)

[2] M.Favata Class. Quantum Grav. 27 084036 (2010)

[3] V.B. Braginsky and K.S. Thorne, Nature (London) 327, 123 (1987)

[4] Zel'Dovich Y B and Polnarev A G 1974 Astron. Zh. 51 30

[5] L.Blanchet, T.Damour, Phy.Rev D 46(10):4304-4319

[6] D.Christodoulou, Phys.Rev.Lett. 67 (1991) 1486-1489

[7] Kilicarslan, E. & Tekin, B. Eur. Phys. J. C (2019) 79: 114

[8] The LIGO Scientific Collaboration et al 2015 Class. Quantum Grav. 32 074001

[9] F.Acernese et al 2015 Class. Quantum Grav. 32 024001

[10] https://dcc.ligo.org/LIGO-T1800044/public

[11] M.Maggiore, *Gravitaional Waves. Volume 1*; Oxford University Press, 2008

[12] K.S.Thorne, Phys.Rev. D 45 520 (1992)

[13] A. D. Johnson, S. J. Kapadia, A. Osborne, A. Hixon, D. Kennefick, Phys. Rev. D 99, 044045 (2019)

[14] https://pycbc.org/

[15] P. D. Lasky, E. Thrane, Y. Levin, J. Blackman, and Y. Chen, Phys. Rev. Lett. 117, 061102 (2016)

[16] https://www.gw-openscience.org/events/GW150914/

[17] https://logbook.virgo-gw.eu/virgo/?r=43891

[18] L. O. McNeill, E. Thrane, P. D. Lasky, Phys. Rev. Lett. 118, 181103 (2017)

[19] M. Favata, Astrophys. J. 696, L159 (2009)

[20] M.Hobson, G.Efstathiou, A.Lasenby; *General Relativity, An Introduction for Physicists*

[21] J.B.Hartle; *Gravity, An Introduction to Einstein's General Relativity*